Bile salt hydrolases shape the bile acid landscape and restrict *C. difficile*

One sentence summary: Bile salt hydrolase activity inhibits *C. difficile* by shaping the conventional and microbial conjugated bile acid pools

Matthew H. Foley[1,2]†, Morgan E. Walker[3]†, Allison K. Stewart[4], Sarah O'Flaherty[2], Emily C. Gentry[5,6], Garrison Allen[1], Shakshi Patel[3], Meichen Pan[2], Violet V. Beaty[3], Caroline Perkins[1], Molly E. Vanhoy[1], Michael K. Dougherty[7], Sarah K. McGill[7], Ajay S. Gulati[8,9], Pieter C. Dorrestein[5,6], Erin S. Baker[4], Matthew R. Redinbo[3,10]*, Rodolphe Barrangou[2]*, Casey M. Theriot[1]*.

1. Department of Pathobiology and Population Health, College of Veterinary Medicine, North Carolina State University, Raleigh, NC, USA

2. Department of Food, Bioprocessing and Nutrition Sciences, North Carolina State University, Raleigh, NC, USA.

3. Department of Chemistry, University of North Carolina at Chapel Hill, Chapel Hill, NC, USA.

4. Department of Chemistry, North Carolina State University, Raleigh, NC, USA

5. Skaggs School of Pharmacy and Pharmaceutical Sciences, University of California San Diego, La Jolla, San Diego, CA, USA

6. Collaborative Mass Spectrometry Innovation Center, Skaggs School of Pharmacy and Pharmaceutical Sciences, University of California San Diego, La Jolla, CA, USA

7. Department of Pediatrics, Division of Gastroenterology and Hepatology, University of North Carolina at Chapel Hill, Chapel Hill, NC, USA

8. Department of Pediatrics, Division of Gastroenterology and Hepatology, University of North Carolina at Chapel Hill, Chapel Hill, NC, USA

9. Department of Pathology and Laboratory Medicine, University of North Carolina at Chapel Hill, Chapel Hill, NC, USA

10. Departments of Biochemistry & Biophysics, and Microbiology & Immunology, and the Integrated Program in Biological and Genome Sciences, University of North Carolina at Chapel Hill, Chapel Hill, NC, USA

† Authors contributed equally to this work

* Corresponding Authors Matthew R. Redinbo redinbo@unc.edu; Rodolphe Barrangou, rbarran@ncsu.edu; Casey M. Theriot, cmtherio@ncsu.edu

Classification

Biological Sciences, Microbiology.

Keywords

bile salt hydrolase, bile acid, microbial conjugated bile acids, live biotherapeutic, *Lactobacillus*, *Clostridioides difficile*

Summary paragraph: Bile acids (BAs) mediate the crosstalk between human and microbial cells and influence intestinal diseases including *Clostridioides difficile* infection (CDI). While bile salt hydrolases (BSHs) shape the BA pool by deconjugating conjugated BAs, the basis for their substrate preferences and impact on *C. difficile* remain elusive. Here, we survey the diversity of *Lactobacillaceae* BSHs and unravel the structural basis of their substrate preference. We show that leveraging BSH activity is an effective strategy to prevent *C. difficile* growth in clinically relevant CDI models. A range of microbial conjugated bile acids (MCBAs) are also identified, comprising unique BSH substrates that also affect multiple aspects of *C. difficile* physiology and pathogenesis. The preferences and efficiency by which BSHs recognize conjugated BAs defines the resulting BA pool, and their ability to variably process the expansive catalogue of MCBAs is a newly prescribed function of BSHs. These findings establish BSHs as intestinal enzymes essential to BA homeostasis, colonization resistance against *C. difficile* and intestinal health.

Introduction

Bile acids (BAs) are host-synthesized and microbial-derived metabolites that support intestinal health and homeostasis by providing a scaffold for host-microbiome crosstalk and adaptation (*1, 2*). Host-encoded BA receptors recognize BAs as signaling molecules to regulate key aspects of host immunity (*3*), metabolism (*4*), and circadian rhythms (*5, 6*). BAs also shape the microbiota, with specific taxa exhibiting resistance to bile stress by harboring mechanisms to survive BA exposure (*7, 8*). The influence of BAs on the microbiota composition is reciprocated by the microbial transformation of BAs to unlock the chemical complexity present in the intestinal BA pool (*9*). The resulting mosaicism of the BA pool is a hallmark of host health and is dependent on the collective activity of microbiome-encoded BA altering enzymes (*10*).

One such enzyme, bile salt hydrolase (BSH), comprises a diverse family of microbial enzymes that catalyze a critical BA transformation step (*11*). Primary conjugated BAs synthesized in the liver, such as the tauro- and glyco- conjugates of cholic acid (TCA, GCA), are deconjugated by BSHs to generate cholic acid (CA) (**Fig. 1A**; BA names and abbreviations are summarized in **Fig. S1**). This vanguard catalytic step acts as a "gatekeeper'' for subsequent BA transformations that turn primary BAs into secondary BAs (*i.e.* deoxycholic acid -DCA- formed from the 7α-dehydroxylation of CA) (*1, 11*).

Dysregulation of BA biosynthesis and BSH activity has been directly implicated in obesity (*12*), cancer (*13*), inflammatory bowel disease (*3*), and colonization resistance against pathogens including *Clostridioides difficile* (*14-18*). Strategically managing BSH activity to rationally toggle BA metabolism and judiciously alter intestinal pathobiology presents an

emerging therapeutic approach. Additionally, the recent discovery of microbial conjugated bile acids (MCBAs) has

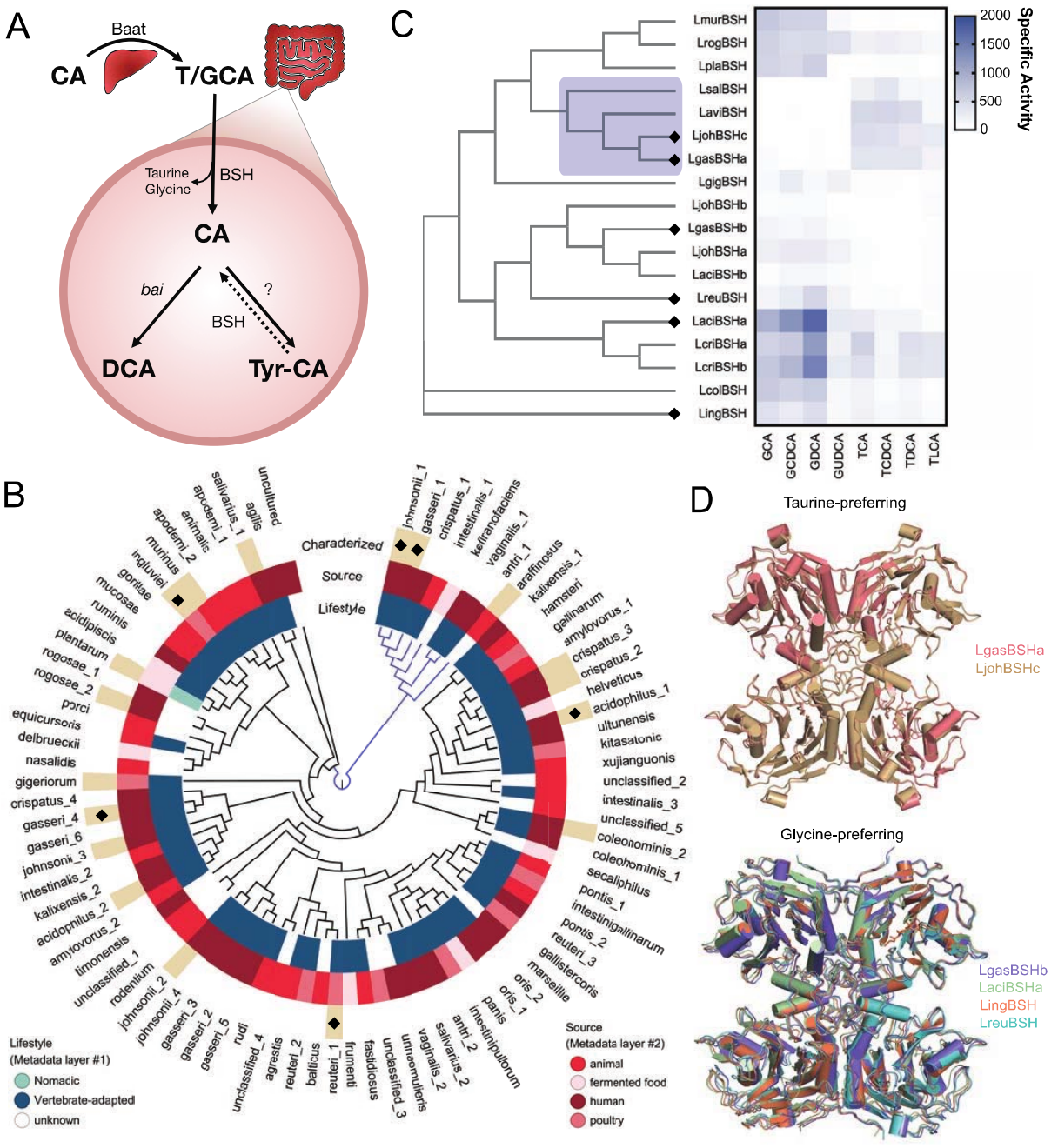

Figure 1. *Lactobacillaceae* BSHs have distinct substrate preferences. (A) Overview of BA metabolism using cholic acid (CA) as an example. BAs are synthesized and conjugated with a taurine or glycine (T/GCA) by the liver enzyme Baat. Conjugated BAs are deconjugated by BSHs, allowing transformations such as 7α-dehydroxylation encoded by the *bai* operon to generate secondary BAs like DCA. Deconjugated BAs can be reconjugated to produce MCBAs like Tyr-CA. (B) The *Lactobacillaceae* BSH phylogenetic tree was assembled from 84 BSH clusters. Major clades are distinguished by branch color. Each cluster name indicates the BSH-encoding species with the inner metadata layers indicating lifestyle and isolation source (*19*). The outer metadata

layer indicates the BSHs cloned for characterization with diamonds indicating BSH crystal structures presented here. (C) Heatmap of BSH activity across conjugated BAs. The clade highlighted in blue displays preference for taurine-conjugated BAs. Values represent mean specific activity (n = 3-4). Phylogenetic relationships between BSHs are based on amino acid sequences. (D) Superposition of the taurine- and glycine-preferring BSH enzyme tetramer crystal structures presented here.

considerably increased the complexity of the BA pool and altered the paradigm of BSH-BA biology, (*20*-*22*) warranting expanded investigations into BSH-substrate relationship (**Fig. 1A**)

Lactobacillaceae species are generally regarded as safe and several strains have been used extensively as probiotics to confer health benefits to the host. Nevertheless, differences in strains, host genetics, and microbiomes have hindered their efficacy (*23*). The rational use and delivery of probiotic-derived products such as BSHs, of which *Lactobacillaceae* harbor a highly active and diverse set (*24*), offers a precision approach to solving this challenge while avoiding concerns such as probiotic engraftment or genetic modification (*25*-*27*).

Here, we examine the phylogenetic, biochemical, and structural diversity and specificity of *Lactobacillaceae* BSHs, a prototypical genus for studying probiotic biology and BA deconjugation. We define how the conjugated amino acid moiety drives substrate preferences in distinct BSHs and how those preferences can be leveraged to prevent *C. difficile* spore germination and colonization in pre-clinical models. We further reveal a new function for BSHs, the ability to deconjugate and reconjugate an expanded set of substrates including MCBAs.

Surveying *Lactobacillaceae* BSH Diversity

To map the range of BSHs harbored by *Lactobacillaceae*, 3,712 genomes from 274 lactobacilli were assembled to comprehensively define the diversity of the enzyme within this genus (**Table S1)** (*28*). Highly similar BSH sequence (>95% amino acid identity) were grouped into 84 clusters and a representative sequence from each cluster was used to construct a

phylogenetic tree. Nearly all BSH clusters were identified from vertebrate-adapted species and ~40% were human-associated, underscoring their role in host-microbiota symbiosis (**Fig. 1B, Table S1**).

To move toward a functional understanding of BSH activity *in vivo*, 18 diverse BSHs were selected for heterologous expression and purification **(Table S2, Fig. S2)**. BSH activity was screened on a panel of conjugated primary and secondary BAs to comprehensively determine BSH substrate preferences **(Fig. 1C)**. We found that BSHs display a clear bias for either glycine or taurine-conjugated BAs. Glycine-preferences dominate the BSHs tested, potentially reflecting the increased abundance of glycine-conjugated BAs among vertebrates (*29*), whereas taurine-specificity is restricted to only a few related BSHs. The glycine-preferring enzyme clade containing LaciBSHa, LcriBSHa, and LcriBSHb exhibits the highest activity. Furthermore, the taurine-preferring LaviBSH, LjohBSHc, and LgasBSHa (corresponding to the clusters arrafinosis, johnsonii_1, and gasseri_1, respectively) enzymes are all present within a single major clade while the LsalBSH (cluster salivarius_1) stands alone in a distantly related branch (**Fig. 1B, C**). This suggests that taurine-preference may have evolved twice within *Lactobacillaceae*. Overall, BSH specialization for glycine or taurine illustrates how lactobacilli may have tailored their metabolism to manage BA exposure.

Defining the structural basis for BSH substrate preference

To examine the molecular foundations of BSH substrate specificity, we determined the crystal structures of six of the BSHs examined above, four that are glycine-preferring (LgasBSHb, LaciBSHa, LingBSH, LreuBSH) and two that are taurine-preferring BSHs (LgasBSHa, LjohBSHc; **Fig. 1D, 2A S3A, Table S3**). LgasBSHa structures were determined in complexes with taurine and taurine plus CDCA; the remaining five structures were unliganded.

All enzymes form analogous tetramers of monomers exhibiting with the core four-layered αββα fold typical of the Ntn-hydrolase family (*30*), with RMSD values ranging from 0.5 to 2.0 Å over equivalent Cα positions (**Fig. 2A, S3B**). Notably, each monomer contains a loop that swaps into the active site of a neighboring monomer within the tetramer (**Fig. 2A-D**). We examined the sequences of these loops and found that taurine-preferring enzymes exclusively contained G-V/T-G motifs while the glycine-preferring enzymes solely contained S-R-G/S motifs (**Fig. 2B, Fig. S4**) (*31*). For both types of enzymes, these unique motifs completed the neighboring active sites by placing amino acids proximal to the catalytic residues (**Fig. 2C-D**). Thus, we hypothesized that these 3-residue motifs play important roles in the glycine vs. taurine substrate preferences of BSH enzymes.

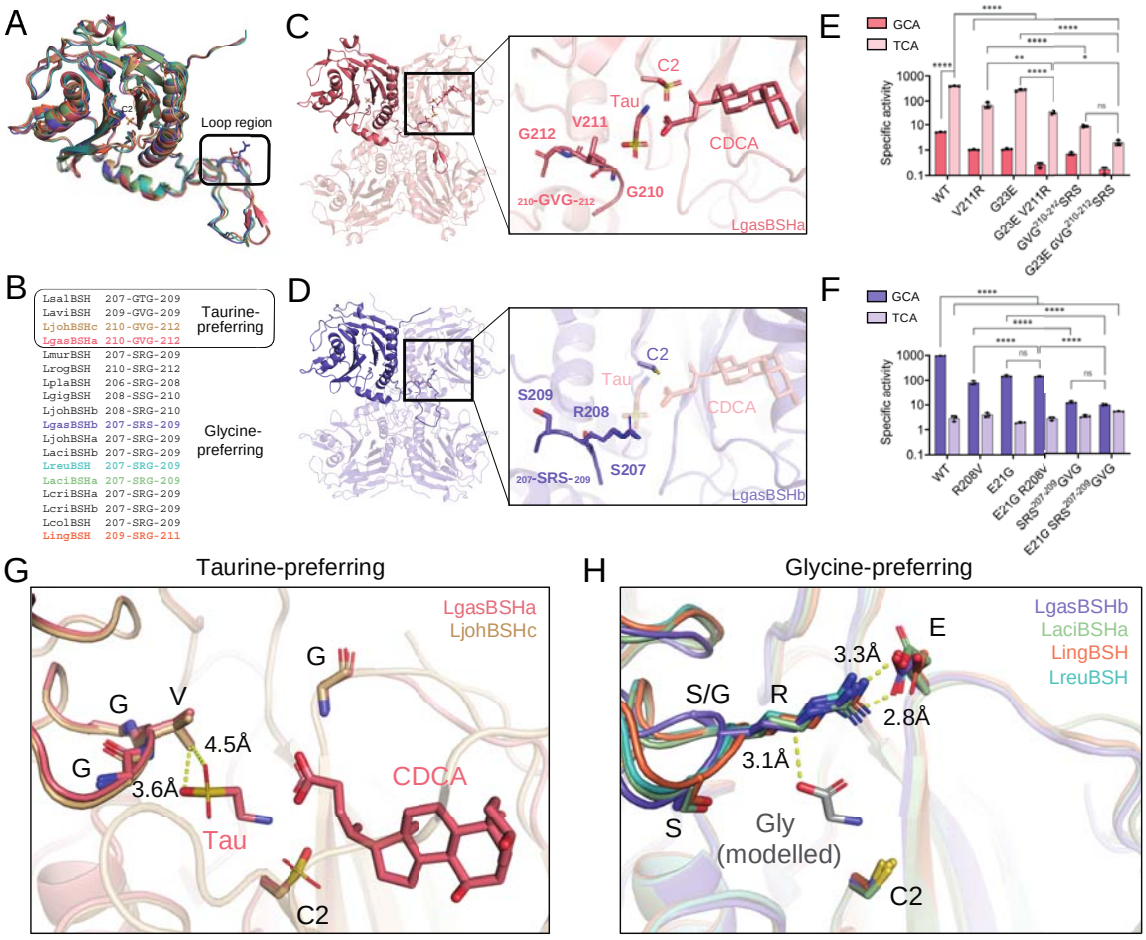

Figure 2. BSH loop region dictates enzyme substrate preference. (A) Superimposed monomers of six BSH structures highlighting the substrate preference loop and colored as indicated in panel B. (B) Sequence alignment of the loop region of *Lactobacillaceae* BSHs. Resolved structures are uniquely colored, with a constant coloring scheme throughout the figure. Taurine-preferring enzymes exhibit a G-V/T-G motif, while glycine-preferring enzymes maintain a S-R-G/S motif. (C) The LgasBSHa tetramer with the active site shown in the inset, where the catalytic cysteine at position 2, the bound taurine and CDCA compounds, and the GVG swapped into the active site from the neighboring monomer are highlighted. (D) The LgasBSHb tetramer with the active site shown in the inset, where the catalytic cysteine at position 2 and the SRS swapped into the active site from the neighboring monomer are highlighted. The taurine and CDCA ligands from the LgasBSHa structure are also rendered transparently. (E) Specific activities for wild-type and mutant forms of LgasBSHa and (F) LgasBSHb with GCA and TCA. Bars in panels E and F are the average of n=3 ± standard deviation. Significant differences were tested by two-way ANOVA with Tukey's multiple comparisons test (ns not significant, $*p < 0.05$, $**p < 0.01$, $****p < 0.0001$). (G) Superposition of the active sites of either two taurine-preferring (G) or four glycine-preferring (H) BSHs structures reveals a consistent active site architecture that accommodates taurine or glycine, respectively.

To test this hypothesis, we first created two variant enzymes that swap the central residues in each motif – a V211R mutant of the taurine-preferring LgasBSHa, and a R208V mutant of the glycine-preferring LgasBSHb – and specific activities with glycine- and taurine-CA conjugates were then examined. We found that both single-swap mutations significantly decreased the specific activities with preferred substrates without significantly impacting the non-preferred substrate (**Fig. 2E, 2F**). Second, we noted that R208 in LgasBSHb forms a salt bridge with E21, an anionic residue conserved in all glycine-preferring enzymes examined; in taurine-preferring BSHs, this glutamate is always replaced by glycine (**Fig. 2G-H**). We tested the importance of these residues by examining the activity of LgasBSHa G23E and LgasBSHb E21G variant proteins. Again, these mutations significantly decreased activity with the preferred substrate without impacting non-preferred substrate activity (**Fig. 2E-F**). Third, combining these mutations by adding a salt bridge in LgasBSHa G23E V211R further lowered the preferred activity more than single mutants (**Fig. 2E**), while removing the salt bridge in LgasBSHb E21G R208V did not further decrease the preferred activity beyond each single mutant (**Fig. 2F**). These data indicate that residues at both positions are crucial for optimal preferential enzyme activity, with the R-E salt bridge conferring an advantage for processing glycine conjugates.

Fourth, we created triple mutants to evaluate the importance of each full 3-residue motif (**Fig. 2C-D**). Both the LgasBSHa-SRS and LgasBSHb-GVG variants exhibited significantly reduced specific activities toward their preferred substrates, and more significant decreases than the single or double mutants, with little effect on non-preferred substrate processing (**Fig. 2E-F**). Finally, adding an additional G/E site change to these 3-residue mutations produced no additional effect (**Fig. 2E-F**). In all cases, variants were confirmed by circular dichroism to have maintained wild-type secondary structure (**Fig. S5**). Furthermore, we observed that the sequence of this 3-residue motif in BSH enzymes from other human gut microbial taxa also correlates with substrate preference, supporting our hypothesis that this region predicts BSH substrate preference (**Fig. S6**). Taken together, these functional data support the structure-guided hypothesis that these 3-residue sequence motifs are predictive of the glycine *vs.* taurine substrate preferences exhibited by *Lactobacillaceae* BSHs.

Bile Acids Inhibit *C. difficile* in a Conjugation-Dependent Manner

C. difficile infection (CDI) is a significant public health problem that can be difficult to treat with conventional antibiotics (*32*). Even after a seemingly successful course of vancomycin or fidaxomicin, there remains a high recurrence rate (~30%) (*33, 34*), making a fecal microbiota transplant (FMT) the last line of treatment (*35*). Although FMTs can be effective for recurrent CDI (rCDI) patients, the long-term consequences remain unclear, making a targeted therapeutic approach appealing for safety and efficacy reasons. Susceptibility to CDI is predominantly driven by antibiotic-driven perturbations to the intestinal microbiota, which results in a loss of colonization resistance (*36, 37*). Strong evidence suggests that microbial BA metabolism is an important mechanism of colonization resistance against *C. difficile* (*38*), as antibiotic usage causes depleted BSHs and increases conjugated BAs (*17*).

BAs govern fundamental aspects of *C. difficile*'s pathogenesis: TCA acts as a germinant for *C. difficile* spores (*39*), whereas CDCA can inhibit germination and growth (*40*). Most studies have focused on the production of deconjugated secondary BAs as inhibitors of *C. difficile* pathogenesis while relatively few have examined the contributions of BSH activity alone (*41*). The therapeutic potential of BSHs has been proposed, but gaps in our knowledge of their pleiotropic effects on intestinal biology and their exact mechanism of action have hampered their development (*42*, *43*).

To determine how BA deconjugation impacts *C. difficile*, we measured the ability of many common BAs to induce spore germination alone or inhibit germination in the presence of a germinant TCA (**Fig. 3A**). While most BAs alone do not induce spore germination in *C. difficile* R20291 (**Fig. S7A**), most BAs tested can inhibit TCA-mediated germination (**Fig. 3B**). Deconjugated BAs are significantly more inhibitory compared to their taurine-conjugated versions whereas they are equally or only mildly more inhibitory relative to their glycine-conjugated variants (**Fig 3B**). We also assayed the ability of BAs to inhibit *C. difficile* growth, as we hypothesized that the conjugation would determine BA toxicity (**Fig. 3C**). Taurine-conjugates inhibit growth less while glycine-conjugates and deconjugated BAs are much more toxic to *C. difficile*. Deconjugated BAs especially inhibit *C. difficile* growth even at low sub-MIC concentrations (**Fig. S8**)**.** These trends mirror the acid-base properties of BAs. Deconjugated BAs are weaker acids, making them more likely to be uncharged and disruptive of the bacterial membrane. Indeed, deconjugated BAs are significantly more disruptive to *C. difficile*'s membrane integrity compared to taurine and glycine-conjugated BAs (**Fig. S7B**). However, conjugated BAs may suppress the expression of *C. difficile*'s toxin A (*tcdA*), as demonstrated using its promoter (P_{tcdA}) fused to an mCherry reporter (**Fig. S7C**). Thus, the use of BSHs to

selectively deconjugate taurine or glycine-conjugated BAs may be able to restrict *C. difficile* in the intestinal tract.

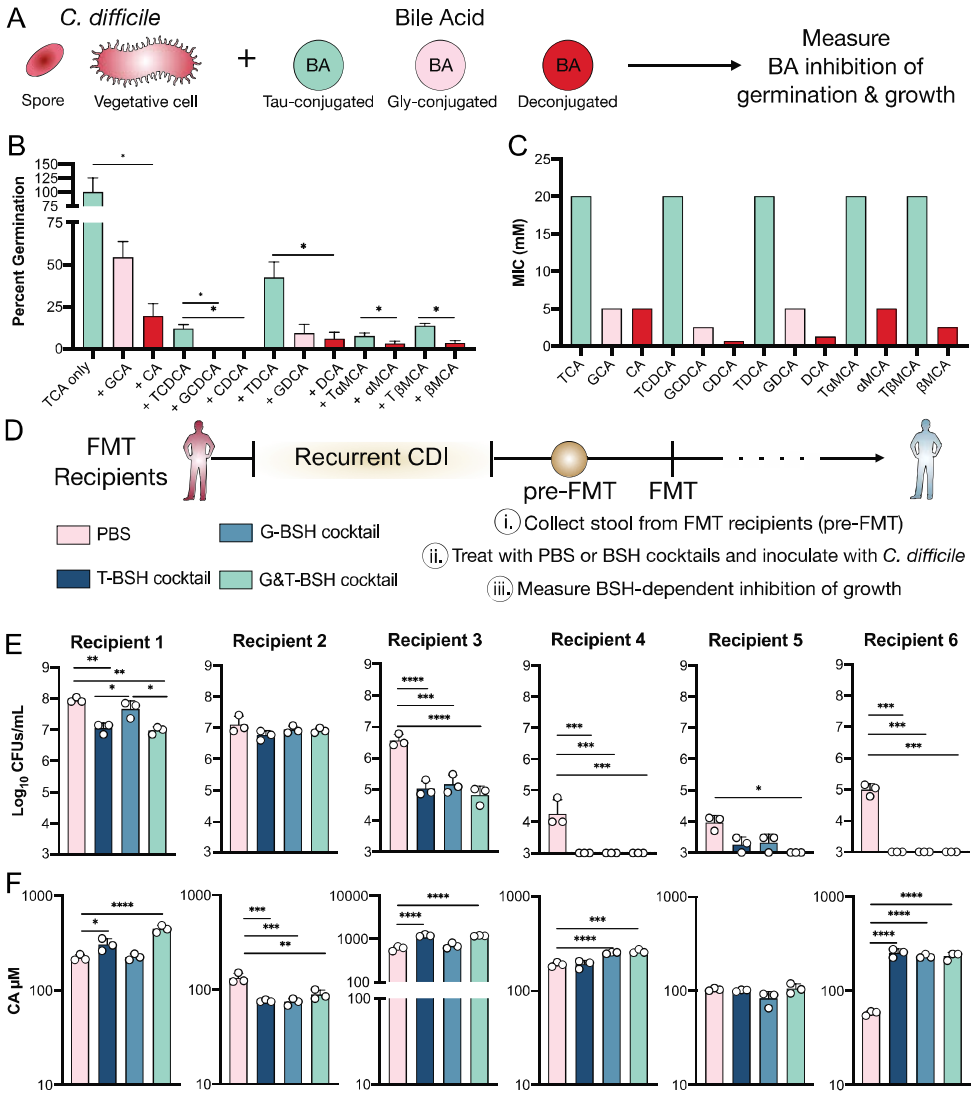

Figure 3. Deconjugated BAs and BSH activity can inhibit *C. difficile*. (A) Schematic of *in vitro* BA-dependent inhibition of *C. difficile* germination and growth. (B) Inhibition of spore germination using various BAs (0.75 mM) in the presence of the germinant TCA (2 mM). (C) Inhibition of *C. difficile* growth as determined by minimum inhibitory concentration (MIC) testing. Statistical differences in B and C were assessed by a one-tailed Welch's *t* test. (D) Schematic of pre-FMT collection and *ex vivo* growth. Pre-FMT stool collected from rCDI patient was supplemented with PBS or a BSH cocktail and subsequently inoculated with *C. difficile*. Recipients 1-3 and 4-6 were inoculated with 10^5 and 10^6 CFUs/mL, respectively. (E) *C. difficile* growth measured at 8h. (F) Targeted metabolomics showing CA from the samples in E. Statistical differences tested by one-way repeated measures ANOVA with Sidak's correction for multiple comparisons. All bars represent the average of n=3 replicates ± sd. **p* < 0.05, ***p* < 0.01, ****p* < 0.001, *****p* < 0.0001.

To determine whether BSH activity and selectivity impacts *C. difficile*, stool from six recurrent CDI (rCDI) patients was collected prior to each receiving an FMT (**Fig 3D**). Unlike mice, FMT recipients have a complex mixture of both taurine and glycine-conjugated BAs (**Fig S9**). Pre-FMT stool was used to culture *C. difficile*, and samples were treated with PBS, a cocktail of taurine-preferring BSHs (T-BSH), glycine-preferring BSHs (G-BSH), or a broadly-acting combination (G&T-BSH) to determine if substrate preference mattered **(Fig. 3E, S9)**. The BSH cocktails, glycine, or taurine alone have no impact on *C. difficile* growth (**Fig. S10**). Despite the pre-FMT stool containing a variety of starting BA pools (**Fig. S9**), virtually all samples displayed BSH-dependent *C. difficile* inhibition at 8 h and/or 24 h regardless of the cocktail's substrate selectivity (**Fig 3E, S11**). Exceptions to this included Recipient 1's stool that only showed inhibition when treated with the T-BSH and G/&T-BSH cocktails, and Recipient 2's stool that showed no inhibition across treatments at 8 h but some inhibition at 24 h (**Fig. 3E, S11**). Recipient 4, 5, and 6's stool all gradually kill *C. difficile* instead of supporting growth, potentially due to antibiotic administration to those patients, but killing was enhanced by all BSH cocktails. Overall, despite the sample heterogeneity across recipients, BSHs appear to effectively hinder *C. difficile* growth, irrespective of their selectivity.

Targeted BA metabolomics was used to validate the activity of the BSH cocktails in stool to examine individual variability between recipients (**Fig 3F, S9**). The stool samples of Recipient 1, 3, 4, and 6 stool displays an increase in deconjugated BAs such as CA primarily in response to the BSH cocktails, thereby supporting the idea that deconjugated BAs can inhibit *C. difficile* (**Fig. S9**). Recipient 3's high concentration of BAs pre-treatment provides an explanation for the robust inhibition observed (**Fig. 3E, S9**). Treatment of Recipient 5's stool with BSHs does not appear to improve deconjugation relative to PBS alone, suggesting that there may be

some basal BSH activity in this sample. Interestingly, Recipient 2 does not display an increase in deconjugated BAs from any BSH treatment, presumably due to the absence of conjugated BAs pre-treatment (**Fig S9**).

BSH Activity Inhibits *C. difficile* Spore Germination and Growth

The observation that BSH treatment can inhibit *C. difficile* in clinically relevant human samples is encouraging, but given the difficulty of controlling for variation across stool samples, we sought to understand how BSHs process BAs in the more controlled environment of the murine intestinal tract. *C. difficile* initiates its infectious cycle when spores arrive and germinate in the small intestine, and then begin to grow and progress to the large intestine where most of the toxin production and disease occurs. To examine the contribution of BSH activity to colonization resistance along the intestinal tract, we collected murine small intestinal and cecal contents from cefoperazone-treated mice at several times post-antibiotic treatment. Content was then supplemented with PBS or the T-BSH cocktail, which can optimally act on the murine BA pool dominated by taurine-conjugated BAs (**Fig. 4A)**. The treated contents were then inoculated with 10^5 spores or CFUs/mL to measure *ex vivo* spore germination and growth, respectively. The addition of the BSH cocktail significantly inhibits *C. difficile* spore germination in the small intestinal contents of all mice and suppresses growth at 8 and 24 h (**Fig. 4B, C)**. Inhibition of growth is more subtle in the cecum, likely due to the lower concentration of conjugated BAs in this region of the intestinal tract (**Fig. 4D, S12**). Targeted metabolomics was used to corroborate the BSH cocktail's effect on the murine BA pool. Small intestinal samples from day 0 treated with the BSH cocktail display a significant increase in deconjugated BAs (CA, CDCA, βMCA, and UDCA) and a decrease in the taurine-conjugated forms of the same BAs. In the cecum, only βMCA was significantly deconjugated (**Fig. 4D, S12**).

Aside from the increase in deconjugated BAs, the most striking difference in the BA pool is the unexpected increase in the MCBAs Ile-CA, Phe-CA, Tyr-CA, Phe-βMCA, and Tyr-βMCA in the BSH-treated small intestinal samples (**Fig 4E**). An array of intestinal bacteria can catalyze the conjugation of BAs to a variety of amino acids through an unknown mechanism (**Fig. 1A**) (*20*, *21*), although no evidence exists at this time that MCBAs can be deconjugated or impact *C. difficile* (*20*). Given the increased CA and βMCA in the BSH-treated samples, these BAs are likely reconjugated by the small intestinal microbiota to produce the MCBAs observed.

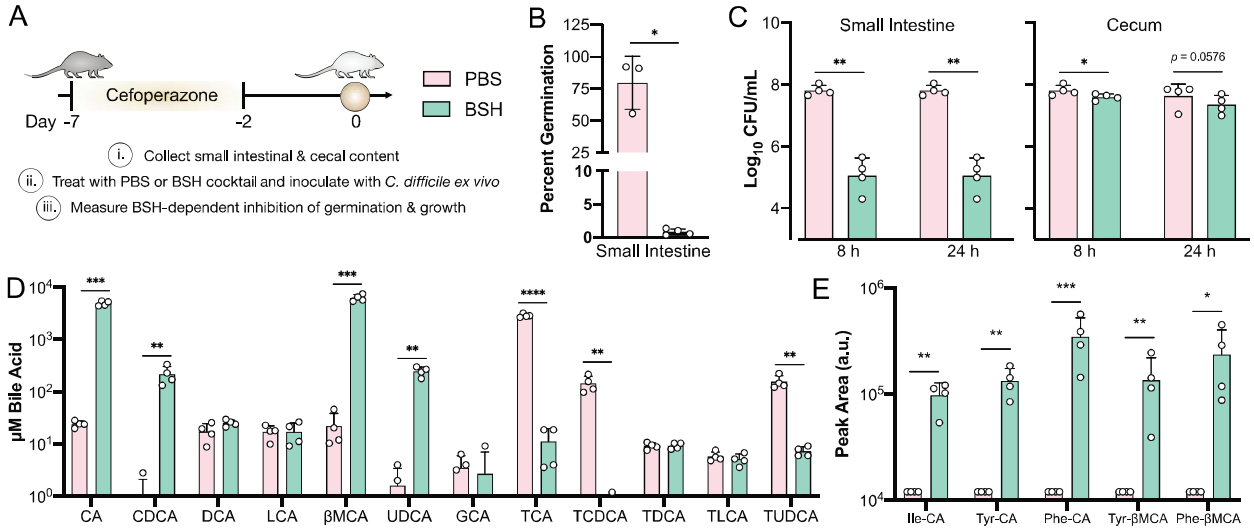

Figure 4. BSHs govern *C. difficile* spore germination and growth along the murine intestinal tract. (A) Schematic of BSH-dependent inhibition of *ex vivo C. difficile* germination and growth. Intestinal contents harvested from cefoperazone-treated mice were supplemented with a cocktail of BSHs and then inoculated with *C. difficile* spores or cells to measure germination or growth, respectively. (B) Germination of *C. difficile* spores in murine small intestinal contents. Contents were treated for 8 h with PBS or a BSH cocktail before inoculation. (C) Growth at 8 and 24 h of *C. difficile* in murine intestinal contents. Contents were treated with PBS or a BSH cocktail and inoculated simultaneously. Statistical differences were tested by ratio paired *t* test. (D, E) Targeted metabolomics showing the BAs identified in the Day 0 small intestinal samples from C. Statistical differences were assessed by one-tailed *t* test. Bars represent mean ± standard deviation. Bars represent mean of n = 4 ± standard deviation. *$p < 0.05$, **$p < 0.01$, ***$p < 0.001$, ****$p < 0.0001$.

BSHs Shape the MCBA Pool and Inhibit *C. difficile*

To further interrogate the role of BSHs in colonization resistance against *C. difficile* and the production of MCBAs *in vivo,* we leveraged the cefoperazone-treated mouse model of

CDI in which the T-BSH cocktail was orally delivered to mice twice daily starting on Day -1 (**Fig. 5A**). Mice were challenged with 10^5 *C. difficile* spores on Day 0 by oral gavage and intestinal content was collected during necropsy at Day 2 to measure the *C. difficile* bacterial burden. Akin to the *ex vivo* results in Figure 4, *C. difficile* growth was significantly inhibited in both the small intestine and the cecum of mice that received the BSH cocktail (**Fig. 5B**). Furthermore, targeted metabolomics of those samples demonstrated that the BSH cocktail remained active *in vivo* and generated a remarkably large proportion of deconjugated BAs despite being orally delivered (**Fig. 5C**). *C. difficile* infection alone resulted in elevated BA deconjugation in mice. While *C. difficile* R20291 strain does not exhibit BSH activity, this is presumably due to dynamic changes in the gut microbiota from CDI.

Given the high concentration of deconjugated BAs generated in the BSH-treated mice (CA, CDCA, βMCA, and UDCA), we hypothesized that a similar set of MCBAs to those seen in **Fig. 4E** would be produced *in vivo*. Indeed, a large and diverse set of MCBAs was observed, with Ile-CA, Tyr-CA, Phe-CA, Arg-CA, and Lys-CA being most prominent (**Fig. 5D, S13)**. Curiously, His-CA was the only MCBA lower in the BSH-treated mice. Together, these results show that BSHs are actively reshaping the MCBA pool, although the catalytic mechanisms involved remain unclear.

To determine whether BSHs can process or display selectivity for specific MCBAs, we screened a larger set of individual BSHs and MCBAs (**Fig. S14**). While activity with MCBAs is relatively low compared to conventional BAs, some BSHs like LingBSH and LreuBSH exhibit appreciable activity. To more broadly examine the recalcitrance of MCBAs, we monitored the deconjugation kinetics of 5 BSHs that had previously exhibited assorted substrate preferences (LingBSH, LgasBSHa, LgasBSHb, LjohBSHc, and LreuBSH) with assorted preferences (**Fig.**

S15A). BSHs were incubated with MCBA pools (AA-CA, AA-CDCA, AA-DCA, and AA-βMCA) that consist of one BA (CA, CDCA, DCA, or βMCA) conjugated to 22 different amino acids, excluding taurine and glycine (*22*), and initial BA deconjugation was quantified using LC-IMS-MS (**Fig. 5E, S15B**). LingBSH displays exceptional activity, suggesting that some BSHs may be uniquely adapted to process this expanded repertoire of BAs (**Fig. 5E, S15B, S16**). Ala- and Ser-conjugated BAs are most efficiently processed, and these observations were validated using purified Ala-CA and Ser-CA demonstrating that their susceptibility to deconjugation is akin to GCA and TCA (**Fig. S14**). Ala and Ser are the smallest amino acids next to Gly, suggesting that the steric constraints of the active site could dictate MCBA deconjugation (**Fig. S17)**. Notably, amine-containing amino acids such as Lys, Gln, and Asn are enriched and among the most efficiently processed conjugates (**Fig. S17**).

We also examined whether MCBA processing would occur in BSH-expressing *L. gasseri* cells. Wild-type, Δ*bshA*, Δ*bshB*, and Δ*bshAB L. gasseri* were incubated with the AA-CDCA pool, and the resultant supernatants were examined to detect deconjugation. We note that the Δ*bshAB* double mutant displays basal deconjugation potentially arising from non-specific hydrolases or cell sequestration of supernatant BAs (**Fig. S15C)**. However, individual BSH activities and substrate preferences were comparably maintained *in vivo*, demonstrating that BSH-expressing bacteria are capable of MCBA deconjugation, and that they do so based on the enzymatic preferences of the BSHs they encode.

Finally, based on the effects conventional BAs have on *C. difficile* pathogenesis, we probed the impact of MCBAs on *C. difficile*. Although none of the tested MCBAs can induce spore germination (**Fig. S18A**)**,** several can inhibit germination including the prominent Tyr-CA, Phe-CA, and Phe-βMCA (**Fig. 5F, S18B**). Additionally, while *C. difficile* growth is enhanced in

the presence of Tyr-CA and Phe-CA, it significantly lags with Tyr-βMCA and Phe-βMCA (**Fig. 5G, S18C**). Thus, the sterol cores of MCBAs distinctly impact the growth of *C. difficile*. It is possible that CA conjugates are relatively poor at disrupting *C. difficile*'s membrane compared to the corresponding conjugates of βMCA, suggesting one potential mechanism for the negative effects of MCBAs on *C. difficile* (**Fig. S7B**). Additionally, several MCBAs suppress P_{tcdA} promoter utilization, indicating that *C. difficile* virulence may also be reduced by the MCBA pool (**Fig. 5H, Fig. S7C**). Together, these results indicate that MCBAs have the capacity to significantly alter the physiology and pathogenesis of *C. difficile*.

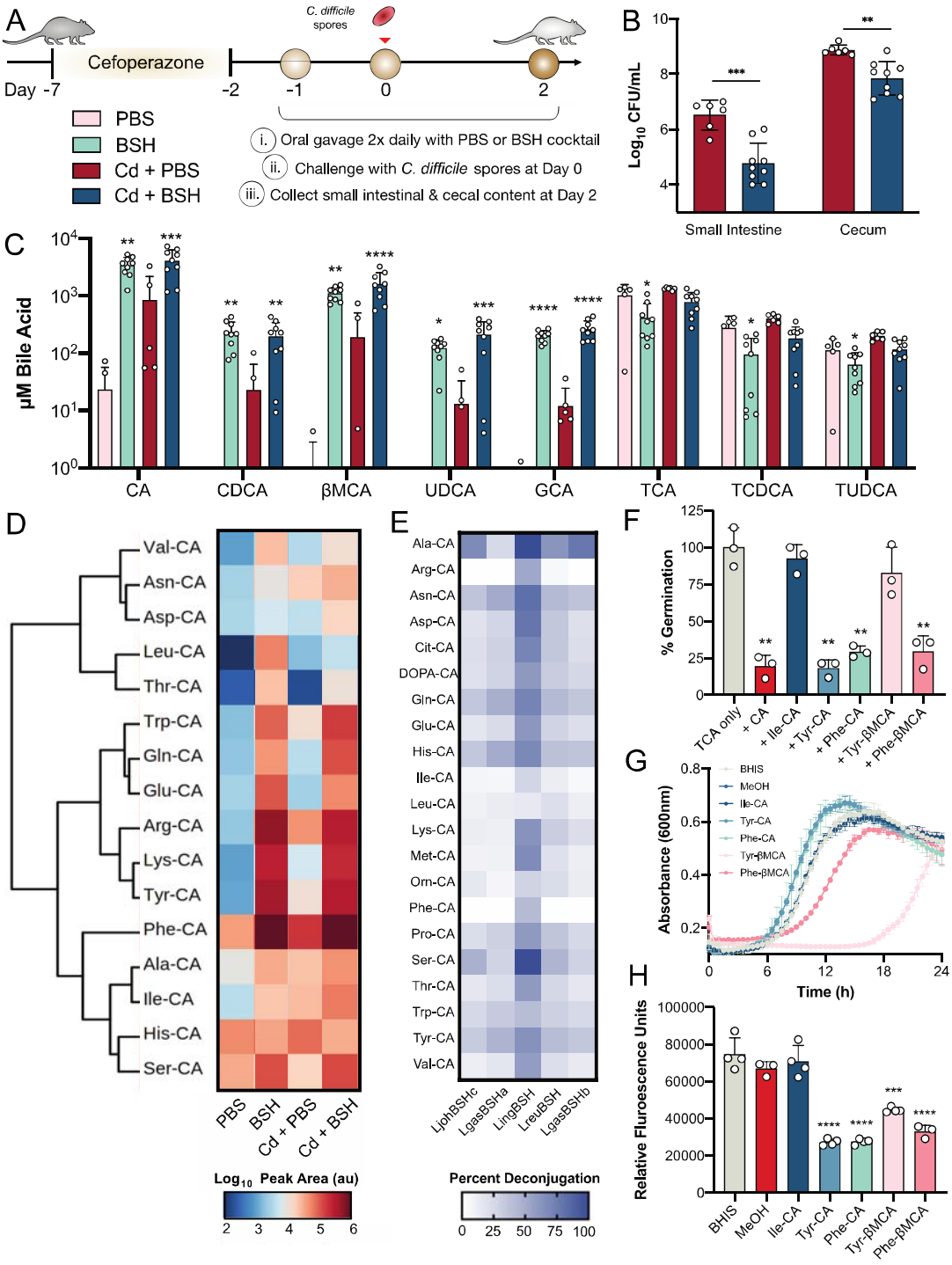

Figure 5. BSHs inhibit *C. difficile* and enriches the MCBA pool *in vivo*. (A) Schematic of BSH delivery in a mouse model of *C. difficile* infection. (B) *C. difficile* CFUs in infected mouse intestinal contents. (C) Targeted metabolomics showing small intestinal BAs from mice in B. (D) Targeted metabolomics showing small intestinal MCBAs identified from mice in B. MCBAs have been Log_{10} transformed and are organized by unsupervised hierarchical clustering. (E) Heatmap of select BSH activity across all MCBA pools. Values represent the mean from n = 3 replicates of % deconjugation after 5 minutes. (F) Inhibition of *C. difficile* germination with MCBAs (0.75 mM) in the presence of the germinant TCA (2 mM). (G) Growth of *C. difficile* in the presence of 0.75

mM MCBAs. (H) MCBA regulation of toxin expression using a P*tcdA*-mCherry reporter. Statistical differences were assessed by one-tailed *t* test. Bars represent mean of n=3-4 ± standard deviation. *$p < 0.05$, **$p < 0.01$, ***$p < 0.001$, ****$p < 0.0001$.

Discussion

There is a growing appreciation for the roles that BSH substrate preferences play in the management of intestinal disease (*6, 8, 44*). This work stresses the distinction between the deconjugation of glycine and taurine-conjugated BAs, the latter of which has been shown to impact the establishment of colonization resistance against *Klebsiella pneumoniae*, the development of colorectal cancer and more recently metabolic disease (*44-46*). Our analysis of *C. difficile*-BA sensitivities motivated our investigation of glycine and taurine-preferring BSHs to inhibit *C. difficile ex vivo* and *in vivo* (**Fig. 3D, 4A, 5A**). Our results suggest that leveraging BA metabolic functions from lactobacilli to restore colonization resistance may present an alternative therapy that avoids antibiotic damage, the unspecified risks of FMTs, and the variability inherent to live biotherapeutics.

The extensive compilation of recently identified MCBAs expands the complexity of the BSH-BA pool and reinforces BSHs as the gatekeepers of bile acid metabolism, capable of reshaping the BA landscape in the gut (*20, 21*). BSH activity fuels the production of MCBAs (**Fig. 4D, 5D**). While the mechanism and purpose of this reconjugation is yet to be elucidated, our observation that MCBAs can inhibit *C. difficile* spore germination and impact growth introduces new mechanistic avenues by which BSH activity can be used to restore colonization resistance after antibiotic treatment (**Fig. 5F, G**). Additionally, these data suggest that BSHs are involved in their production. Actually, work investigating BSH-catalyzed reconjugation is underway (once the preprints are available from the Quinn and Patterson labs, we will provide the citations here). Furthermore, our demonstration that BSHs exhibit variable propensities for

MCBA substrates supports a model in which BSHs directly shape the production and decomposition of the MCBA pool, and further bolsters their use as a precision tool to modulate BA metabolism *in vivo* (**Fig. 4E, S15**).

Lactobacillaceae are associated with BSH activity *in vivo* (*47, 48*). BSHs perform the important role of BA deconjugation and reconjugation, and perturbations to this process are implicated in several diseases including CDI, which currently lacks effective strategies for prevention and intervention (*49*). *C. difficile* physiology and pathogenesis is exceptionally responsive to alterations in BSH activity, thereby establishing these enzymes as a potential targeted approach to restore colonization resistance. The preferences and efficiency by which BSHs recognize conjugated BAs defines the resulting BA pool, and their ability to variably process the expansive catalogue of MCBAs is a newly prescribed function of BSHs, with implications for human intestinal health and disease.

References

1. M. H. Foley, S. O'Flaherty, R. Barrangou, C. M. Theriot, Bile salt hydrolases: Gatekeepers of bile acid metabolism and host-microbiome crosstalk in the gastrointestinal tract. *PLoS Pathog* **15**, e1007581 (2019).
2. C. L. Gentile, T. L. Weir, The gut microbiota at the intersection of diet and human health. *Science* **362**, 776-780 (2018).
3. A. Lavelle, H. Sokol, Gut microbiota-derived metabolites as key actors in inflammatory bowel disease. *Nat Rev Gastroenterol Hepatol* **17**, 223-237 (2020).
4. S. N. Chaudhari *et al.*, Bariatric surgery reveals a gut-restricted TGR5 agonist with anti-diabetic effects. *Nat Chem Biol* **17**, 20-29 (2021).
5. K. Govindarajan *et al.*, Unconjugated bile acids influence expression of circadian genes: A potential mechanism for microbe-host crosstalk. *PLoS One* **11**, e0167319 (2016).
6. L. Yao *et al.*, A selective gut bacterial bile salt hydrolase alters host metabolism. *Elife* **7**, (2018).
7. K. B. Islam *et al.*, Bile acid is a host factor that regulates the composition of the cecal microbiota in rats. *Gastroenterology* **141**, 1773-1781 (2011).
8. M. H. Foley *et al.*, *Lactobacillus* bile salt hydrolase substrate specificity governs bacterial fitness and host colonization. *Proc Natl Acad Sci U S A* **118**, (2021).
9. J. M. Ridlon, S. C. Harris, S. Bhowmik, D. J. Kang, P. B. Hylemon, Consequences of bile salt biotransformations by intestinal bacteria. *Gut Microbes* **7**, 22-39 (2016).
10. B. Jia, D. Park, Y. Hahn, C. O. Jeon, Metagenomic analysis of the human microbiome reveals the association between the abundance of gut bile salt hydrolases and host health. *Gut Microbes* **11**, 1300-1313 (2020).
11. J. M. Ridlon, D. J. Kang, P. B. Hylemon, Bile salt biotransformations by human intestinal bacteria. *J Lipid Res* **47**, 241-259 (2006).
12. S. A. Joyce *et al.*, Regulation of host weight gain and lipid metabolism by bacterial bile acid modification in the gut. *Proc Natl Acad Sci U S A* **111**, 7421-7426 (2014).
13. C. Ma *et al.*, Gut microbiome-mediated bile acid metabolism regulates liver cancer via NKT cells. *Science* **360**, (2018).
14. S. L. Burgess *et al.*, Gut microbiome communication with bone marrow regulates susceptibility to amebiasis. *J Clin Invest* **130**, 4019-4024 (2020).
15. S. Alavi *et al.*, Interpersonal Gut Microbiome Variation Drives Susceptibility and Resistance to Cholera Infection. *Cell* **181**, 1533-1546 e1513 (2020).
16. K. H. Wilson, Efficiency of various bile salt preparations for stimulation of Clostridium difficile spore germination. *J Clin Microbiol* **18**, 1017-1019 (1983).
17. C. M. Theriot *et al.*, Antibiotic-induced shifts in the mouse gut microbiome and metabolome increase susceptibility to *Clostridium difficile* infection. *Nat Commun* **5**, 3114 (2014).
18. B. H. Mullish *et al.*, Microbial bile salt hydrolases mediate the efficacy of faecal microbiota transplant in the treatment of recurrent *Clostridioides difficile* infection. *Gut* **68**, 1791-1800 (2019).
19. R. M. Duar *et al.*, Lifestyles in transition: evolution and natural history of the genus *Lactobacillus*. *FEMS Microbiol Rev* **41**, S27-S48 (2017).
20. R. A. Quinn *et al.*, Global chemical effects of the microbiome include new bile-acid conjugations. *Nature* **579**, 123-129 (2020).

21. L. N. Lucas *et al.*, Dominant bacterial phyla from the human gut show widespread ability to transform and conjugate bile acids. *mSystems*, e0080521 (2021).
22. E. Gentry *et al.*, https://www.researchsquare.com/article/rs-820302/v1. *Nature Portfolio*, (2022).
23. J. C. Sniffen, L. V. McFarland, C. T. Evans, E. J. C. Goldstein, Choosing an appropriate probiotic product for your patient: An evidence-based practical guide. *PLoS One* **13**, e0209205 (2018).
24. Z. Song *et al.*, Taxonomic profiling and populational patterns of bacterial bile salt hydrolase (BSH) genes based on worldwide human gut microbiome. *Microbiome* **7**, 9 (2019).
25. J. Claesen, M. A. Fischbach, Synthetic microbes as drug delivery systems. *ACS Synth Biol* **4**, 358-364 (2015).
26. E. S. Shepherd, W. C. DeLoache, K. M. Pruss, W. R. Whitaker, J. L. Sonnenburg, An exclusive metabolic niche enables strain engraftment in the gut microbiota. *Nature* **557**, 434-438 (2018).
27. E. Koh *et al.*, Engineering probiotics to inhibit Clostridioides difficile infection by dynamic regulation of intestinal metabolism. *Nat Commun* **13**, 3834 (2022).
28. S. O'Flaherty, A. Briner Crawley, C. M. Theriot, R. Barrangou, The *Lactobacillus* bile salt hydrolase repertoire reveals niche-specific adaptation. *mSphere* **3**, (2018).
29. G. A. Nagana Gowda, N. Shanaiah, A. Cooper, M. Maluccio, D. Raftery, Bile acids conjugation in human bile is not random: new insights from (1)H-NMR spectroscopy at 800 MHz. *Lipids* **44**, 527-535 (2009).
30. F. Xu *et al.*, The complex structure of bile salt hydrolase from *Lactobacillus salivarius* reveals the structural basis of substrate specificity. *Sci Rep* **9**, 12438 (2019).
31. F. Madeira *et al.*, The EMBL-EBI search and sequence analysis tools APIs in 2019. *Nucleic Acids Res* **47**, W636-W641 (2019).
32. C. Slimings, T. V. Riley, Antibiotics and hospital-acquired *Clostridium difficile* infection: update of systematic review and meta-analysis. *J Antimicrob Chemother* **69**, 881-891 (2014).
33. O. A. Cornely, M. A. Miller, T. J. Louie, D. W. Crook, S. L. Gorbach, Treatment of first recurrence of *Clostridium difficile* infection: fidaxomicin versus vancomycin. *Clin Infect Dis* **55 Suppl 2**, S154-161 (2012).
34. S. Polivkova, M. Krutova, V. Capek, B. Sykorova, J. Benes, Fidaxomicin versus metronidazole, vancomycin and their combination for initial episode, first recurrence and severe Clostridioides difficile infection - An observational cohort study. *Int J Infect Dis* **103**, 226-233 (2021).
35. C. R. Kelly *et al.*, Effect of fecal microbiota transplantation on recurrence in multiply recurrent *Clostridium difficile* infection: A randomized trial. *Ann Intern Med* **165**, 609-616 (2016).
36. R. C. Owens, Jr., C. J. Donskey, R. P. Gaynes, V. G. Loo, C. A. Muto, Antimicrobial-associated risk factors for *Clostridium difficile* infection. *Clin Infect Dis* **46 Suppl 1**, S19-31 (2008).
37. R. A. Britton, V. B. Young, Role of the intestinal microbiota in resistance to colonization by *Clostridium difficile*. *Gastroenterology* **146**, 1547-1553 (2014).

38. A. D. Reed, C. M. Theriot, Contribution of nhibitory metabolites and competition for nutrients to colonization resistance against *Clostridioides difficile* by Commensal Clostridium. *Microorganisms* **9**, (2021).
39. J. A. Sorg, A. L. Sonenshein, Bile salts and glycine as cogerminants for *Clostridium difficile* spores. *J Bacteriol* **190**, 2505-2512 (2008).
40. J. A. Sorg, A. L. Sonenshein, Chenodeoxycholate is an inhibitor of *Clostridium difficile* spore germination. *J Bacteriol* **191**, 1115-1117 (2009).
41. R. Thanissery, J. A. Winston, C. M. Theriot, Inhibition of spore germination, growth, and toxin activity of clinically relevant *C. difficile* strains by gut microbiota derived secondary bile acids. *Anaerobe* **45**, 86-100 (2017).
42. M. L. Jones, C. Tomaro-Duchesneau, C. J. Martoni, S. Prakash, Cholesterol lowering with bile salt hydrolase-active probiotic bacteria, mechanism of action, clinical evidence, and future direction for heart health applications. *Expert Opin Biol Ther* **13**, 631-642 (2013).
43. S. A. Joyce, F. Shanahan, C. Hill, C. G. Gahan, Bacterial bile salt hydrolase in host metabolism: Potential for influencing gastrointestinal microbe-host crosstalk. *Gut Microbes* **5**, 669-674 (2014).
44. B. J. Russell *et al.*, Intestinal transgene delivery with native E. coli chassis allows persistent physiological changes. *Cell*, (2022).
45. A. Stacy *et al.*, Infection trains the host for microbiota-enhanced resistance to pathogens. *Cell* **184**, 615-627 e617 (2021).
46. J. M. Ridlon, P. G. Wolf, H. R. Gaskins, Taurocholic acid metabolism by gut microbes and colon cancer. *Gut Microbes* **7**, 201-215 (2016).
47. F. Li *et al.*, Microbiome remodelling leads to inhibition of intestinal farnesoid X receptor signalling and decreased obesity. *Nat Commun* **4**, 2384 (2013).
48. A. Knarreborg, R. M. Engberg, S. K. Jensen, B. B. Jensen, Quantitative determination of bile salt hydrolase activity in bacteria isolated from the small intestine of chickens. *Appl Environ Microbiol* **68**, 6425-6428 (2002).
49. X. Na, C. Kelly, Probiotics in clostridium difficile Infection. *J Clin Gastroenterol* **45 Suppl**, S154-158 (2011).

Acknowledgements: This work was performed in part by the Molecular Education, Technology and Research Innovation Center (METRIC) at NC State University, which is supported by the State of North Carolina.

Funding: We thank IFF for supporting this study. MHF was supported by the University of North Carolina Center for Gastrointestinal Biology and Disease postdoctoral fellowship training grant T32DK07737. MEW was supported through the NIH training grant T32GM008570 and NSF DGE-1650116. This study was also supported by R01 GM135218 and GM137286; NIEHS P30 ES025128, P42 ES027704, and P42 ES031009; and the Environmental Protection Agency

STAR RD 84003201 award. The FMT study was supported by the NCTraCS Translational and Clinical Sciences Institute Pilot Grant UNCSUR11609. MD was supported by NIH training grant T32 DK007634.

Author contributions: MHF, MEW, SOF, ECP, MRR, RB, CMT designed the research. MHF, MEW, AKS, SOF, ECG, GA, SP, MP, CP, VVB, MEV, PCD, and ESB performed, analyzed, and interpreted experiments. SOF and MP performed bioinformatic analysis of BSHs. MHF and GA performed BSH specific activity assays and *C. difficile* experiments. MEW, SP, and VVB performed crystallographic/structural work and activity assays. MKD, SKM, and ASG collected patient samples. AKS performed metabolomic analyses. ECG synthesized non-canonical bile acids. MF and MEW wrote the manuscript which all authors edited.

Competing interests: MRR is a Founder of Symberix, Inc., and the recipient of research funding from Merck and Lilly, although those funds were not used in this project. PCD is a scientific advisor to Cybele and is a co-founder and scientific founder of Ometa and Enveda, with prior approval by UC-San Diego.

CMT consults for Vedanta Biosciences, Inc., Summit Therapeutics, and Ferring Pharmaceuticals, Inc. CMT is a founder of CRISPR Biotechnologies. RB is a founder of Ancilia Biosciences and CRISPR Biotechnologies. MHF, SOF, RB and CMT are inventors on a patent application related to the use of *Lactobacillus* BSH enzymes.

Data and materials availability: All data associated with this study are available in the main text or the Supplementary Materials. All LC-IMS-MS data are publicly available on Panorama under the Panorama dashboard of the Baker Lab-NCSU within the “0821 BSH Assessment”, “1121 Mouse Germination and Growth Ex-Vivo” and the “1121 Theriot FMT Ex-Vivo Growth” projects."

List of Supplementary materials:

Materials and Methods

Fig S1 to S19

Table S1 to S4